



# Carbonized $\pi$ -conjugated polymer-coated porous silica: preparation and evaluating its extraction ability for berberine

Pian Jin<sup>1</sup> · Fucheng Zhu<sup>2</sup> · Mi Jiang<sup>1</sup> · Makoto Takafuji<sup>3</sup> · Hirotaka Ihara<sup>3</sup> · Lei Nie<sup>1</sup> · Houmei Liu<sup>1</sup>

Received: 31 August 2022 / Accepted: 12 September 2022 / Published online: 3 October 2022  
© The Author(s), under exclusive licence to Springer-Verlag GmbH Austria, part of Springer Nature 2022

## Abstract

In view of the limitations of existing berberine solid-phase extraction adsorbents, this paper proposes a novel carbonized  $\pi$ -conjugated polymer-coated porous silica ( $\text{SiO}_2$ @C- $\pi$ -CP) adsorbent with simple process and low cost for efficient extraction of berberine by multiple interactions. Characterization methods, including Brunner–Emmet–Teller measurement, thermogravimetric analysis, X-ray photoelectron spectroscopy, and scanning electron microscopy techniques, were used to verify the successful modification of carbonized  $\pi$ -conjugated polymer on the surface of porous silica. The berberine was selected as target molecule, and the adsorption mechanism and process were investigated through adsorption kinetics, adsorption isotherms, and thermodynamic studies. The fitting results show that the adsorption of berberine by  $\text{SiO}_2$ @C- $\pi$ -CP well conforms to the pseudo-second-order and Langmuir models. By optimizing the main SPE parameters, the SPE method based on  $\text{SiO}_2$ @C- $\pi$ -CP was developed. Excellent results were obtained, including low limit of detection ( $0.75 \text{ ng mL}^{-1}$ ) and limit of quantification ( $2 \text{ ng mL}^{-1}$ ), wide linearity ( $2\text{--}13,000 \text{ ng mL}^{-1}$ ), and satisfactory relative standard deviations (RSD) of inter-day (1.5%) and intra-day (6.2%). Finally, the  $\text{SiO}_2$ @C- $\pi$ -CP also has been successfully used to the enrichment of berberine in real urine samples. This research makes clear that  $\text{SiO}_2$ @C- $\pi$ -CP has outstanding potential for trace enrichment of berberine alkaloids.

**Keywords** Berberine · Solid-phase extraction · Adsorbent · Carbonized polymer · Urine analysis

## Introduction

Berberine is a natural isoquinoline alkaloid mainly extracted from the rhizomes of *Coptidis Rhizoma* [1, 2]. For now, the activities of berberine that have been found include antidiarrheal [3], antibacterial [4], antiviral [5], antimalarial [6], antitumor [7], hypoglycemic [8], hypolipidemic [9, 10], anti-inflammatory, and anti-angiogenic [11, 12]. With the

advantages of extensive natural sources [13, 14], it has a very broad therapeutic prospect and is already one of the most commonly used alkaloid drugs in clinical practice. Therefore, it is necessary to realize the efficient determination of berberine and its metabolites in complex biological matrices. This makes it an urgent need to develop a user-friendly efficient pre-treatment method for complex berberine body fluid samples.

Solid-phase extraction (SPE) has been a powerful and widely used sample pretreatment technology due to its unique features, such as high recovery, short extraction time, high enrichment factor, low organic solvents consumption, and ease of automation [15]. In the procedure of SPE, the type of sorbent plays an important role to obtain higher enrichment efficiency of analytes [16].

The combination of novel high-efficiency adsorbents and SPE technology may have become a powerful method to determine the content of berberine in complex matrices. Many efforts have been made in related areas. For example, Zhu et al. [15] developed a novel type of PAA-PZNs adsorbent, combined with a non-aqueous SPE process to efficiently enrich alkaloids. Then, in order to quickly separate

✉ Lei Nie  
nielei2004@sdu.edu.cn

✉ Houmei Liu  
hmliu@sdu.edu.cn

<sup>1</sup> Key Lab of Chemical Biology (MOE), School of Pharmaceutical Sciences, Shandong University, Jinan 250012, Shandong, China

<sup>2</sup> Medical Science and Technology Innovation Center, Shandong First Medical University, Jinan 250117, Shandong, China

<sup>3</sup> Faculty of Advanced Science and Technology, Kumamoto University, 2-39-1 Kurokami, Chuo-ku, Kumamoto 860-8555, Japan

alkaloids isomers from green tea, Li et al. [17] designed a novel DESs-Fe<sub>3</sub>O<sub>4</sub>/MIPs adsorbent. In combination with magnetic solid-phase extraction technology, this adsorbent performed very well in the pretreatment process of green tea samples. Also, in Hu's work [18], a magnetic sorbent (Ni@POFs) with high extraction effect was synthesized for the preconcentration and determination of trace alkaloids in human urine. Although all the adsorbents mentioned above have quite good analytical results, most of their synthesis processes are complicated and their commercialization potential is poor.

About the research of isolating and purifying berberine alkaloids from complex systems, our group selected four quaternary ammonium alkaloids (QAAs: coptisine chloride, sanguinarine, berberine chloride, and chelerythrine) as analytes and also did a related work. In that study, a double carboxyl silicane modified graphene oxide coated silica composite (TSPSAcide@GO@SiO<sub>2</sub>) [19] was successfully designed, which has satisfactory extraction performance for QAAs. However, the synthesis steps of TSPSAcide@GO@SiO<sub>2</sub> is equally complicated as those existing adsorbents, and the foreseeable high-cost future inevitably limits the promotion of TSPSAcide@GO@SiO<sub>2</sub>. Thus, it is still a very meaningful work to develop a berberine alkaloids adsorbent with an economic synthetic process.

In 2017, Hirota Ithara et al. reported a novel  $\pi$ -conjugated polymer ( $\pi$ -CP) [20], which is rich in polar functional groups and conjugated structures, having strong multiple interactions with berberine alkaloids [19, 21–23]. Also, in theory,  $\pi$ -CP can be coated on any desired carrier surface [24, 25], which makes its application range no longer limited. Most importantly, the synthesis of  $\pi$ -CP is fairly simple. It only requires two monomers to react in ethanol (or any other suitable solvent) at 80 °C for 10 h, without additional catalyst, without high temperature and high pressure. So, we planned to deposit  $\pi$ -CP onto the surface of mesoporous silica, obtaining  $\pi$ -conjugated polymer-coated porous silica composite (SiO<sub>2</sub>@ $\pi$ -CP), for berberine adsorption. SiO<sub>2</sub>@ $\pi$ -CP would have both polar groups and conjugated structure, which makes it have strong multiple interactions with berberine. However, after  $\pi$ -CP modification, part of the pore structures on the silica support were to be masked, resulting in a decrease in the effective adsorption area.

In the same year in 2017, another work published by Hirota Ithara's research group [26] mentioned that heat treatment (200–560 °C) would eliminate the polar groups on the surface of  $\pi$ -CP and form long-range  $\pi$ -conjugated structures. Also, the higher the temperature, the richer the long-range  $\pi$ -conjugated structure formed. When the carbonization temperature is higher than 560 °C, the polar groups are basically no longer eliminated. Heat treatment is a very common processing method in material synthesis

[27–29], often shrinking the material and giving it better stability. Therefore, SiO<sub>2</sub>@ $\pi$ -CP was finally carbonized for superior performance. This is because high-temperature heating would enrich the conjugated structure of the  $\pi$ -CP shell and shrink it, weakening the cover of the pores and correspondingly increasing the effective action sites.

In short, for the analysis of trace berberine in body fluids, a carbonized  $\pi$ -conjugated polymer-coated porous silica (SiO<sub>2</sub>@C- $\pi$ -CP) was designed based on a very economical modifier. Urine was selected as the actual sample matrix to evaluate the anti-interference and practicability ability of SiO<sub>2</sub>@C- $\pi$ -CP. The effect of heat treatment on material properties will also be briefly explored by analyzing the characterization results. Finally, by this work, the application potential of  $\pi$ -conjugated polymers would be further developed and it also opened up new ideas for efficient pre-treatment of trace berberine alkaloids in complex matrices.

## Experimental

### Reagents

The Stöber silica particles used as the coating matrix were obtained from Welch Materials, Inc. (Tianjin, China, <http://www.welchmat.com>); their diameter, specific surface area, pore volume, and pore size are 20–40  $\mu\text{m}$ , 321  $\text{m}^2 \text{g}^{-1}$ , 0.82  $\text{mL g}^{-1}$ , and 102 Å, respectively. The Purifier FST-IV-10 Ultra-Pure Water System (18.2  $\text{M}\Omega\cdot\text{cm}$  at 25 °C) used throughout the experiments was produced by Shanghai Fushite Instrument Equipment Co., Ltd. (Shanghai, China, <http://fstyqsb.com>). The SPE blank column tubes and polyethylene cribriform plates used to pack adsorbent were purchased from Shenzhen Comma Biotechnology Co., Ltd.; the column volume is 3 mL and the sieve pore size is 10  $\mu\text{m}$ . Two commercial SPE cartridges, silica SPE cartridge and C18 SPE cartridge, used in preliminary adsorption quantity comparison experiment were also provided by Shenzhen Comma Biotechnology Co., Ltd. (Shenzhen, China, <http://www.biocomma.cn>). Two monomers, 1,5-dihydroxynaphthalene (DHN, > 99%) and 1,3,5-trimethylhexahydro-1,3,5-triazine (TMTA, > 98%), used for polymerization were purchased from Tokyo Chemical Industry Co., Ltd. (Shanghai, China, <https://www.tcichemicals.com/CN/zh/>). Berberine chloride hydrate ( $\geq 95\%$ ) was provided by Aladdin Chemical Reagent Co., Ltd. (Shanghai, China, <https://www.aladdin-e.com>). The acetonitrile used for HPLC analysis was provided by Oceanpak Company (Sweden). Triethylamine, phosphoric acid (H<sub>3</sub>PO<sub>4</sub>), and sodium hydroxide were all obtained from Sinopharm Chemical Reagent Co., Ltd. (Shanghai, China, <https://www.sinoreagent.com>).

## Apparatus

All HPLC tests were completed on Agilent 1260 HPLC system equipped with a quaternary pump and diode array detector (Agilent, USA). The ZNCL-GS intelligent magnetic stirrer, purchased from Zhengzhou Ketai Laboratory Equipment Co., Ltd. (Zhengzhou, China, <http://www.zzketai.com>), was used to synthesize the adsorbent material. All the SPE processes involved in this work were completed on the SPE 80 semi-automatic solid-phase extraction system (Hanon Advanced Technology Group Co., Ltd, Jinan, China, <http://www.hanon.cc>). ASAP 2020/TriStar 3000 (Micromeritics) apparatus (USA), Gemini SEM 300 electron microscope (Carl Zeiss Microscopy GmbH), TGA Q50 (USA), and PHI 5000 Versaprobe II (VP-II) electron spectrometer (Ulvac-Phi) were used to obtain the N<sub>2</sub> adsorption–desorption isotherm (BET), scanning electron microscopy (SEM), thermogravimetric analysis (TGA), and X-ray photoelectron spectroscopy (XPS) data in material characterization section, respectively. There are some instruments used during sample processing, including KQ-3200DE ultrasonic cleaning machine (Kunshan Ultrasonic Instrument Co., Ltd., Jiangsu, China, <http://www.ks-csyq.com>), TGL-16C Benchtop High Speed Centrifuge (Shanghai Anting Scientific Instrument Factory, Shanghai, China, <http://www.centrifuge.com.cn>), and DZF-6050 vacuum drying oven (Shanghai Jinghong Experimental Equipment Co., Ltd., Shanghai, China, <http://jinghongsh.com>).

## Preparation of carbonized $\pi$ -conjugated polymer modified silica composite (SiO<sub>2</sub>@C- $\pi$ -CP)

As shown in Scheme 1, first, ultrasonic treatment was used to completely disperse the silica matrix (1.0 g), DHN (5 mM),

and TMTA (5 mM) in 100 mL ethanol. The dispersion was refluxed for 10 h at 80 °C under magnetic stirring. When reaction was finished, the obtained  $\pi$ -conjugated polymer modified silica composite (SiO<sub>2</sub>@ $\pi$ -CP) was washed with ethanol several times and dried under vacuum at 50 °C for 12 h.

Then, the dried SiO<sub>2</sub>@ $\pi$ -CP was heat-treated at 560 °C for 2 h in a nitrogen atmosphere, obtaining the resultant carbonized  $\pi$ -conjugated polymer modified silica composite (SiO<sub>2</sub>@C- $\pi$ -CP).

## Preparation of standard solution

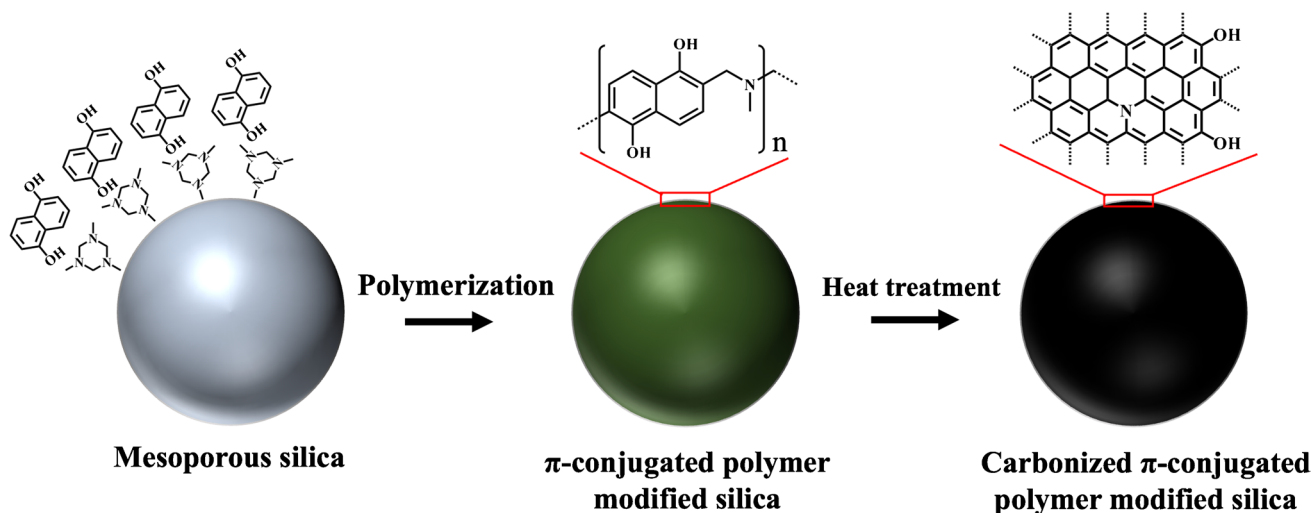
The berberine chloride hydrate was dissolved with methanol to prepare a standard stock solution of 500  $\mu\text{g mL}^{-1}$ , stored in a refrigerator at 4 °C. This stock solution was used after being diluted with pure water during the subsequent experiments.

## SPE procedure

In the first step, a polyethylene sieve plate was placed at the bottom of the blank column tube, and 50 mg dried SiO<sub>2</sub>@C- $\pi$ -CP was loaded, and then another plate was used to block the upper end of the compacted packing. Under the optimized extraction conditions (summarized in Table S1), the final eluents were first vacuum dried, then re-dissolved with 100  $\mu\text{L}$  50% ethanol solution (volume ratio), and finally analyzed by HPLC.

## Batch adsorption studies

First, 20 mL of berberine solutions with different initial concentrations were prepared, adding 50 mg SiO<sub>2</sub>@C- $\pi$ -CP adsorbent



**Scheme 1** Schematic illustration showing the preparation procedures of SiO<sub>2</sub>@C- $\pi$ -CP

to each. After dispersing, incubating, and centrifugation, the adsorption tests were finished by the detection of the supernatants. The calculation of the specific adsorption capacity of the  $\text{SiO}_2@\text{C}-\pi\text{-CP}$  for berberine is abided by  $Q=(C_0-C_e)\times V$ .  $Q$  represents rebinding capacity on 50 mg  $\text{SiO}_2@\text{C}-\pi\text{-CP}$  adsorbent,  $C_0$  and  $C_e$  are the concentrations of berberine at initial time and equilibrium time, and  $V$  is the volume of sample solution.

In this research, all experimental data were tested repeatedly three times, and the calculated average value was taken as the final data.

### Application of $\text{SiO}_2@\text{C}-\pi\text{-CP}$ in human urine samples

All human urine used in experiments was provided by healthy volunteers. First, the collected human urine was filtered and stored at 4 °C for later use. When using, first rewarm the low-temperature urine to room temperature, add berberine standard solution to prepare a berberine urine sample with a certain concentration, and then test according to the “SPE procedure” section. Finally, the recovery is calculated according to the following formula:

$$\text{Recovery} = (C_{\text{test}}V_{\text{eluent}})/(C_{\text{add}}V_{\text{loading}}) \times 100$$

Here,  $C_{\text{test}}$  is the concentration of the eluate detected by HPLC and  $V_{\text{eluent}}$  is the volume of eluent.  $C_{\text{add}}$  and  $V_{\text{loading}}$  are the known concentration and volume of the loaded berberine urine sample solution, respectively.

### Chromatographic conditions

The column used to analyze berberine was ChromCore 120 C18 (dimension  $4.6 \times 150$  mm, 5  $\mu\text{m}$ ). The HPLC mobile

phase consisted of ACN (35%) and 1% triethylamine buffer (65%,  $\text{H}_3\text{PO}_4$  adjusted the pH to 3). The flow rate, column temperature, and DAD detector wavelength of the 1260 HPLC system were 1.0  $\text{mL min}^{-1}$ , 30 °C, and 345 nm, respectively. The injection volume of the sample was 20  $\mu\text{L}$ .

## Results and discussion

### Characterization of $\text{SiO}_2@\text{C}-\pi\text{-CP}$

The experimental data of nitrogen adsorption–desorption shown in Fig. 1a and Table S2 can provide specific surface area and pore structure information of  $\text{SiO}_2$ ,  $\text{SiO}_2@\pi\text{-CP}$ , and  $\text{SiO}_2@\text{C}-\pi\text{-CP}$ . For  $\text{SiO}_2$ , the H1-type mesoporous hysteresis loop, which represents the existence of capillary condensation step, appears at the relative pressures ( $P/P_0$ ) of 0.6–0.9, corresponding to a total pore volume of  $\sim 0.82$   $\text{cm}^3 \text{g}^{-1}$  and a pore size of 9.0–12.0 nm ( $\sim 10$  nm). Due to the modification of  $\pi\text{-CP}$  on silica surface, the capillary condensation step of  $\text{SiO}_2@\pi\text{-CP}$  exists in a lower  $P/P_0$  range (0.6–0.85) with the decrease of pore volume ( $\sim 0.82$   $\text{cm}^3 \text{g}^{-1}$  drops to  $\sim 0.66$   $\text{cm}^3 \text{g}^{-1}$ ), pore size ( $\sim 10$  nm drops to  $\sim 5.8$  nm), and specific surface area ( $337$   $\text{m}^2 \text{g}^{-1}$  drops to  $281$   $\text{m}^2 \text{g}^{-1}$ ). For  $\text{SiO}_2@\text{C}-\pi\text{-CP}$ , undergone heat treatment, the size shrinkage occurs, resulting in the increase of specific BET surface area ( $281$   $\text{m}^2 \text{g}^{-1}$  rises to  $321$   $\text{m}^2 \text{g}^{-1}$ ), pore volume ( $\sim 0.66$   $\text{cm}^3 \text{g}^{-1}$  rises to  $\sim 0.80$   $\text{cm}^3 \text{g}^{-1}$ ), and pore size ( $\sim 5.8$  nm rises to  $\sim 7.2$  nm). These sandwiched data for  $\text{SiO}_2@\text{C}-\pi\text{-CP}$  show that an approximately 0.9-nm-thick  $\text{C}-\pi\text{-CP}$  shell was formed on the surface of silica. Also, the  $\pi\text{-CP}$  modification did partially block the pores in  $\text{SiO}_2$ ;

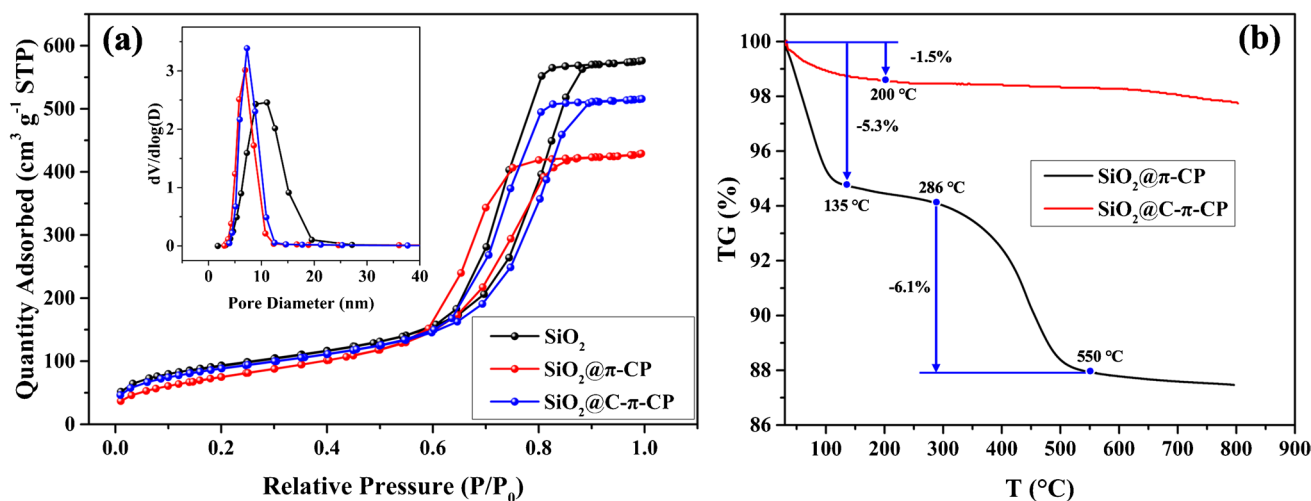


**Fig. 1**  $\text{N}_2$  adsorption–desorption isotherm and pore size distribution (inset) of  $\text{SiO}_2$ ,  $\text{SiO}_2@\pi\text{-CP}$ , and  $\text{SiO}_2@\text{C}-\pi\text{-CP}$  (a). The thermogravimetric analysis curves of  $\text{SiO}_2@\pi\text{-CP}$  and  $\text{SiO}_2@\text{C}-\pi\text{-CP}$  (b)

heat treatment can effectively solve the problem of channel blockage accordingly, as we expected.

The results of thermogravimetric analysis in the range of 0–800 °C are shown in Fig. 1b. For  $\text{SiO}_2@ \pi\text{-CP}$ , during the heat treatment progress, first stage, the remaining solvent or physically adsorbed water rapidly release (5.3% weight loss). Subsequently,  $\pi\text{-CP}$  shell starts to carbonize and shrink, resulting in apparent weight loss (−6.1%). In stark contrast, the weight loss curve of  $\text{SiO}_2@ \text{C-}\pi\text{-CP}$  tends to be flat except for the slight mass loss starting from 0 to 200 °C (−1.5%), which is most likely due to the physically adsorbed water. This is because  $\text{SiO}_2@ \text{C-}\pi\text{-CP}$  was obtained from  $\text{SiO}_2@ \pi\text{-CP}$  after heat treatment at 560 °C and naturally has better thermal stability.

X-ray photoelectron spectroscopy (XPS) is used to obtain the information about the elemental composition, chemical status, and molecular structure on the material surface. The XPS characteristics of  $\text{SiO}_2@ \pi\text{-CP}$  and

$\text{SiO}_2@ \text{C-}\pi\text{-CP}$  are shown in Fig. 2a and b, the characteristic peaks of  $\text{N}_{1s}$  (401 eV) and  $\text{C}_{1s}$  (285.5 eV) are from the modified  $\pi\text{-CP}$  and  $\text{C-}\pi\text{-CP}$ , and the peak of  $\text{O}_{1s}$  (533 eV) is from  $\text{SiO}_2$  core and  $\pi\text{-CP}/\text{C-}\pi\text{-CP}$ . Comparing the set of data, the peak intensity of  $\text{O}_{1s}$  and  $\text{N}_{1s}$  decreased, and  $\text{C}_{1s}$  increased. However, because the dominant sector of  $\text{SiO}_2@ \pi\text{-CP}$  and  $\text{SiO}_2@ \text{C-}\pi\text{-CP}$  is  $\text{SiO}_2$ , the element content changes are not obvious. So, the second set of data for pure  $\pi\text{-CP}$  and  $\text{C-}\pi\text{-CP}$  are also conducted. From Fig. 2c and d, the data indicate that after heat treatment, the content of  $\text{O}_{1s}$  and  $\text{N}_{1s}$  of  $\text{C-}\pi\text{-CP}$  obviously decreased and the content of  $\text{C}_{1s}$  evidently increased. These two sets of data all explained that heat treatment promotes cyclization accompanied by elimination of nitrogen and oxygen to form long-range  $\pi$ -conjugated structure, resulting in the increasing of carbon content [26]. Compared with  $\pi\text{-CP}$ , that is, the  $\text{C-}\pi\text{-CP}$  modified layer has more abundant conjugated structures.

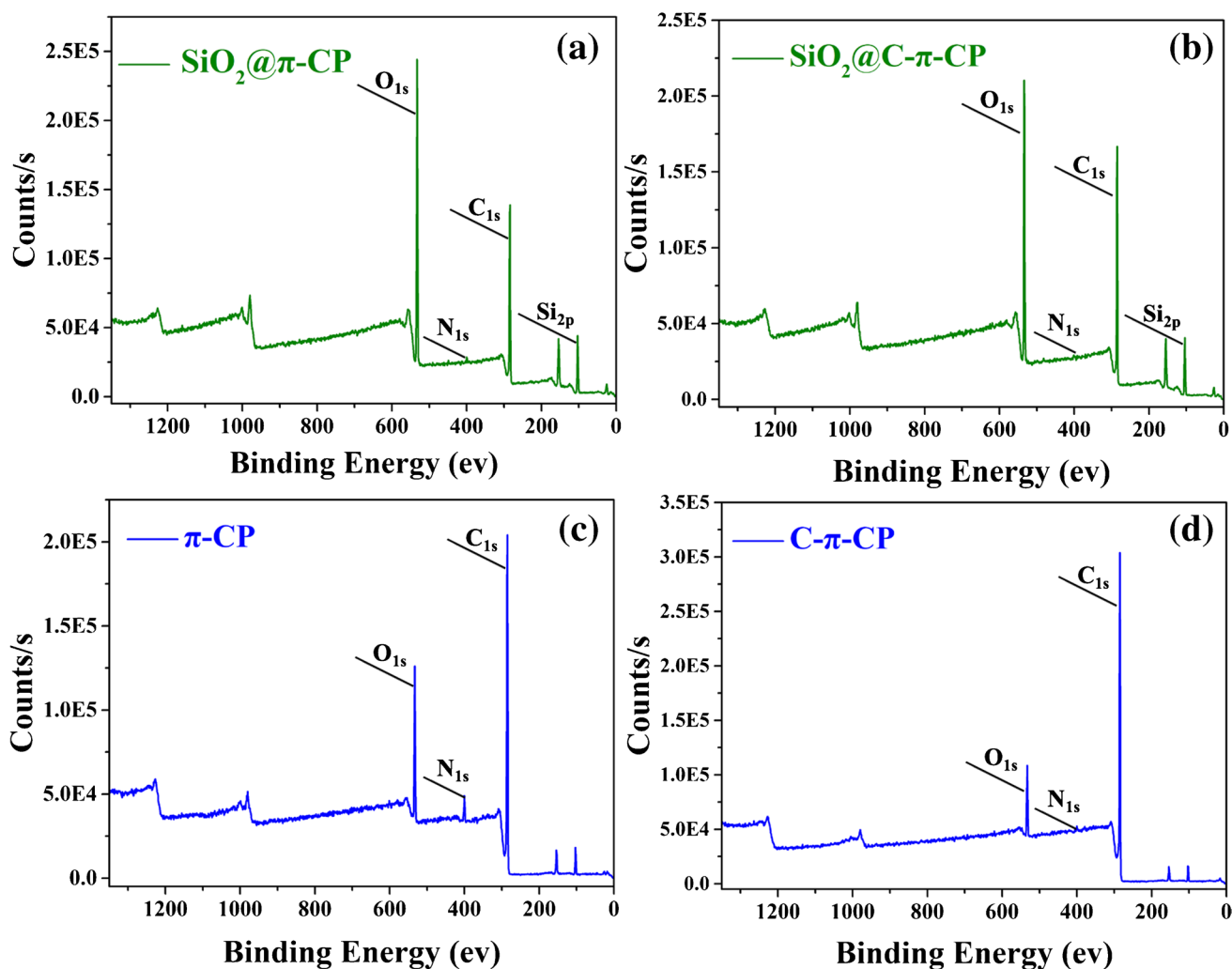


Fig. 2 The X-ray photoelectron spectroscopy of  $\text{SiO}_2@ \pi\text{-CP}$  (a),  $\text{SiO}_2@ \text{C-}\pi\text{-CP}$  (b),  $\pi\text{-CP}$  (c), and  $\text{C-}\pi\text{-CP}$  (d)



The SEM is used to investigate the size, dispersibility, surface topography of  $\text{SiO}_2@\text{C}-\pi\text{-CP}$ , and the changes before and after heat treatment. It can be seen from Fig. S1 that the particle sizes of  $\text{SiO}_2@\text{C}-\pi\text{-CP}$  and  $\text{SiO}_2@\pi\text{-CP}$  are basically the same. This is because the polymer shell covered on the surface is very thin (only about 0.9 nm on average) compared with the  $\text{SiO}_2$  core (20–40  $\mu\text{m}$ ). A significant change is the polymer surface of  $\text{SiO}_2@\text{C}-\pi\text{-CP}$  that is smoother and tighter than that of  $\text{SiO}_2@\pi\text{-CP}$ , which can be ascribed to the shrinkage of modification layer after high-temperature treatment.

### Determination of saturated adsorption capacity

In order to estimate whether the adsorption capacity of  $\text{SiO}_2@\pi\text{-CP}$  had changed significantly after carbonization, the saturated adsorption capacity of  $\text{SiO}_2@\pi\text{-CP}$  and  $\text{SiO}_2@\text{C}-\pi\text{-CP}$  to berberine was investigated, respectively. Also, two commonly used commercial SPE cartridges, silica SPE cartridge and C18 SPE cartridge, were tested to initially assess the commercialization potential of  $\text{SiO}_2@\text{C}-\pi\text{-CP}$ . The details of the two commercial SPE cartridges are shown in Table S3 and the saturated adsorption capacity comparison results are shown in Fig. 3. The adsorption capacity of  $\text{SiO}_2@\text{C}-\pi\text{-CP}$  (14.2  $\mu\text{g mg}^{-1}$ ) to berberine is much higher than that of  $\text{SiO}_2@\pi\text{-CP}$  (8.6  $\mu\text{g mg}^{-1}$ ), which has been better than that of the two commercial SPE cartridges (3.9  $\mu\text{g mg}^{-1}$  and 7.3  $\mu\text{g mg}^{-1}$ ). It can be preliminarily determined that the adsorption capacity of  $\text{SiO}_2@\pi\text{-CP}$  is significantly improved after carbonization and  $\text{C}-\pi\text{-CP}$  modified silica-based adsorbent has excellent commercialization potential. It is so convenient that just by adding a simple heat treatment process, the conjugated structure of  $\pi\text{-CP}$  can

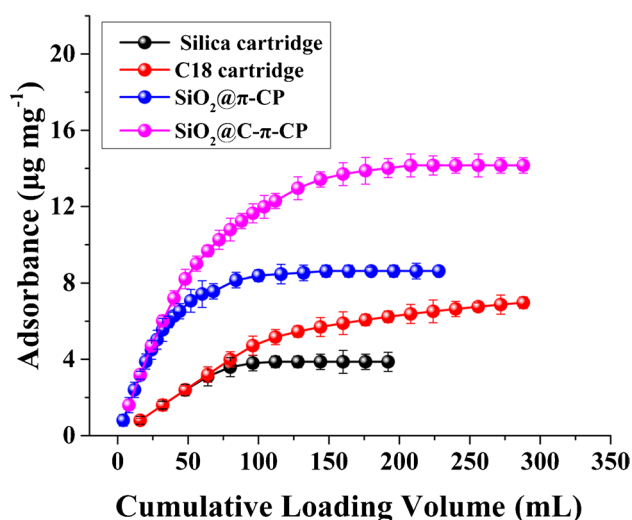


**Fig. 3** The saturated adsorption capacity of commercial silica cartridge, C18 cartridge,  $\text{SiO}_2@\pi\text{-CP}$ , and  $\text{SiO}_2@\text{C}-\pi\text{-CP}$  to berberine

be significantly increased, the polymer modified layer can be tightened, more adsorption sites are released, and the adsorption advantages of  $\pi\text{-CP}$  can be further exerted.

### Adsorption kinetics

The kinetic study of the adsorption process is mainly used to describe the rate of the adsorbent that adsorbs the adsorbate, and the data is fitted through the kinetic models, so as to explore its adsorption mechanism. Figure 4d describes the adsorption kinetics of berberine on  $\text{SiO}_2@\text{C}-\pi\text{-CP}$  with different initial concentrations. It clearly shows that as the initial concentration increases, the adsorption capacity increases. Moreover, they all can achieve adsorption equilibrium within 30 min. This is because in the initial stage of adsorption, there are a large number of unoccupied sites, and gradually, the binding sites are saturated, and finally the adsorption equilibrium is reached.

In this work, three classic dynamical models were used to fit the experimental data. Their equations are given as

$$\text{Pseudo - first - order model } \ln(q_e - q_t) = \ln q_e - K_1 t \quad (1)$$

$$\text{Pseudo - second - order model } t/q_t = 1/(K_2 q_e^2) + t/q_e \quad (2)$$

$$\text{Intra - particle diffusion model } q_t = K_{id} t^{0.5} + C \quad (3)$$

Here,  $q_t$  ( $\text{mg g}^{-1}$ ) and  $q_e$  ( $\text{mg g}^{-1}$ ) are the adsorption capacity of berberine by the adsorbents in real time  $t$  (h) and at the adsorption equilibrium, respectively;  $K_1$  ( $\text{h}^{-1}$ ),  $K_2$  ( $\text{g mg}^{-1} \text{h}^{-1}$ ), and  $K_{id}$  ( $\text{g mg}^{-1} \text{h}^{-1/2}$ ) are the kinetic rate constants of the corresponding models, respectively.  $C$  ( $\text{mg g}^{-1}$ ) is a constant related to thickness and boundary layer.

The fitting curves are displayed in Fig. 4a, b, and c. The above-mentioned kinetic parameters and correlation coefficients obtained from model fitting are summarized in Table 1. It can be seen that under different initial concentrations, the correlation coefficients obtained by linear fitting using the pseudo-second-order model all reach 0.999, which are significantly higher than that of pseudo-first-order model (0.558–0.972) and intra-particle diffusion model (0.960–0.982). Moreover, the  $q_e$  values obtained by the pseudo-second-order model fitting are well consistent with the data measured in the actual experiment. So, the pseudo-second-order kinetic model provides the best correlation with experimental data among the three kinetic models, indicating that during the adsorption process, there was electron sharing or electron transfer between  $\text{SiO}_2@\text{C}-\pi\text{-CP}$  and berberine in aqueous media [30].

The intra-particle diffusion model is used to confirm the mass transfer steps. Shown in Fig. 4c, the piecewise linear regression of the data shows that there are two steps in the entire adsorption process: adsorption on the surface of the adsorbent and diffusion in the pores. The two straight lines

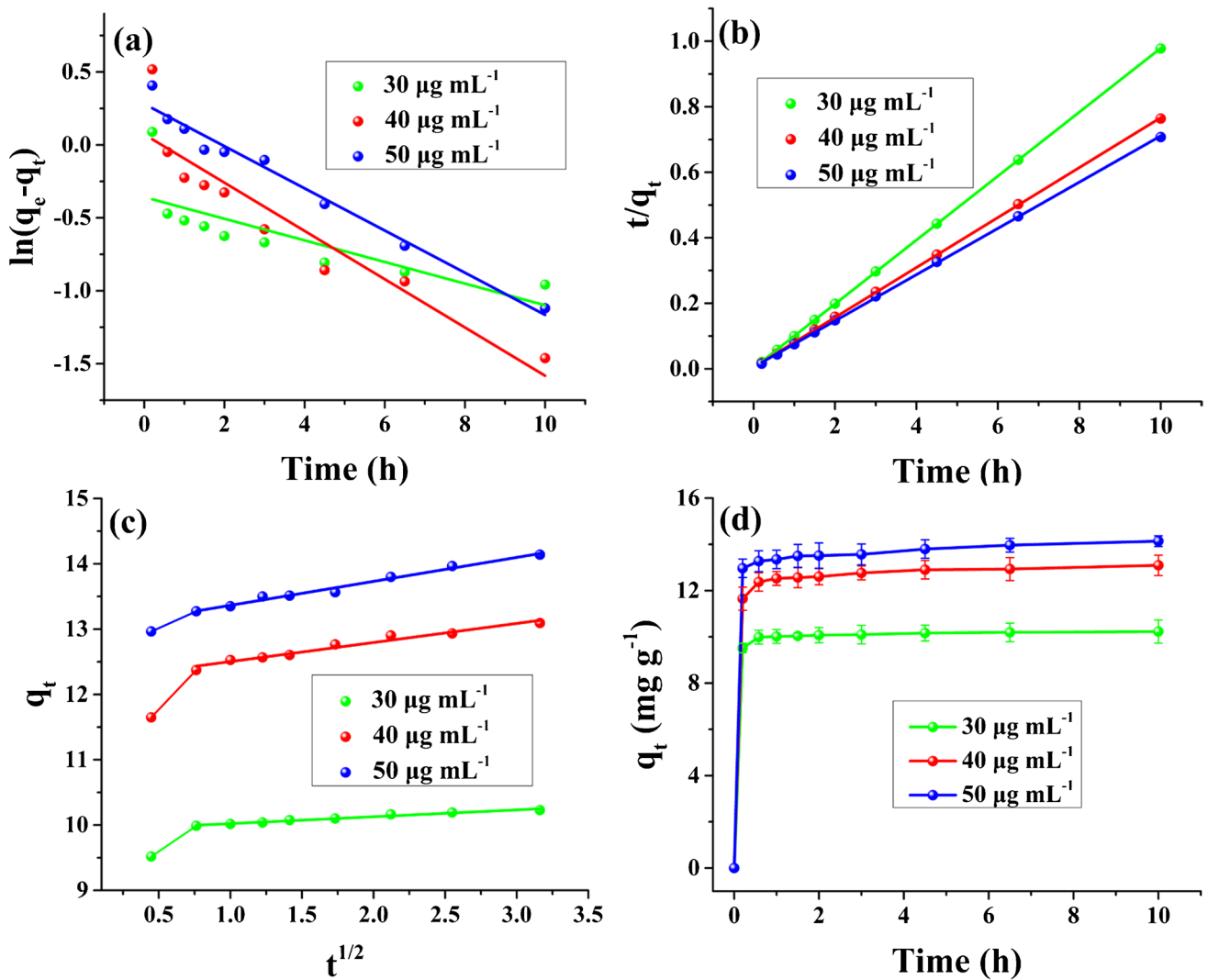


**Fig. 4** The adsorption kinetics of berberine at different concentrations onto SiO<sub>2</sub>@C-π-CP fitted by pseudo-first-order model (a), pseudo-second-order model (b), and intra-particle diffusion model (c). Effect

of contact time on the adsorption of berberine at different initial concentrations onto SiO<sub>2</sub>@C-π-CP (d)

do not pass through the origin, indicating that internal diffusion is not the only step to control the adsorption process.

### Adsorption isotherms

The adsorption isotherms describe the equilibrium relations between adsorbent and adsorbate at a certain temperature. In this study, three frequently used adsorption isotherm models, namely, the Langmuir, Freundlich, and Temkin models, were used to fit the adsorption isotherm of berberine on SiO<sub>2</sub>@C-π-CP. Their mathematical equations are described as follows:

$$\text{Langmuir model } c_e/q_e = c_e/q_{max} + 1(K_L q_{max}) \quad (4)$$

$$\text{Freundlich model } \ln q_e = (\ln c_e)/n + \ln K_F \quad (5)$$

$$\text{Temkin model } q_e = RT \ln(K_T c_e)/b_T \quad (6)$$

In the above equations, q<sub>e</sub> (mg g<sup>-1</sup>) is the amount of berberine adsorbed by adsorbent at the equilibrium time, c<sub>e</sub> (mg L<sup>-1</sup>) is the concentration of berberine in the equilibrated solution, q<sub>max</sub> (mg g<sup>-1</sup>) is the theoretical maximum amount for adsorbing berberine on a single layer of adsorbent, and K<sub>L</sub> (L mg<sup>-1</sup>) is the Langmuir constant which is related to the adsorption free energy. K<sub>F</sub> (mg g<sup>-1</sup> (mg L<sup>-1</sup>)<sup>-1/n</sup>) and 1/n are the Freundlich constants which indicate the adsorption capacity and the adsorption intensity, respectively [31]. Also, the smaller the value of 1/n, the better the adsorption performance of the adsorbent [32]. R (8.314 J mol<sup>-1</sup> K<sup>-1</sup>) is

**Table 1** Parameters of different kinetic models at different concentrations for berberine adsorption on SiO<sub>2</sub>@C- $\pi$ -CP

Initial concentrations (mg L <sup>-1</sup> )	$q_e$ , exp (mg g <sup>-1</sup> )	Pseudo-first-order			Pseudo-second-order			Interparticle diffusion				
		$q_e$ (mg g <sup>-1</sup> )	$K_1$ (mg g <sup>-1</sup> h <sup>-1</sup> )	$R^2$	$q_e$ (mg g <sup>-1</sup> )	$K_2$ (g mg <sup>-1</sup> h <sup>-1</sup> )	$R^2$	$K_{id1}$ (mg g <sup>-1</sup> h <sup>-1/2</sup> )	C1	$K_{id2}$ (mg g <sup>-1</sup> h <sup>-1/2</sup> )	C2	$R^2$
30	10.611	0.699	0.074	0.558	10.245	3.663	0.999	1.493	8.849	0.105	9.916	0.968
40	13.325	1.075	0.165	0.853	13.123	1.319	0.999	2.304	10.618	0.292	12.210	0.960
50	14.466	1.324	0.144	0.972	14.184	0.974	0.999	0.983	12.524	0.367	12.997	0.982

the ideal gas constant,  $T$  (K) is the incubation temperature,  $K_T$  (L g<sup>-1</sup>) is the Temkin isotherm constant, and  $b$  (kJ mol<sup>-1</sup>) is the constant related to the heat of sorption [33, 34].

The fitting results are summarized in Table 2 and Fig. 5. In the comprehensive comparison of the correlation coefficients, it can be seen that the Langmuir equation is better than the Freundlich and Temkin models for describing the adsorption behavior of berberine hydrochloride on SiO<sub>2</sub>@C- $\pi$ -CP. It indicates that the adsorption of berberine by SiO<sub>2</sub>@C- $\pi$ -CP is monolayer adsorption. The adsorption capacity of the adsorbent is limited by the number of sorption sites and all sorption sites are equivalent and isolate from each other [35].

As can see from Fig. 5d, the amount of berberine adsorbed on SiO<sub>2</sub>@C- $\pi$ -CP increased with the increase of the initial berberine concentration and decreased with the increase of temperature. Namely, low temperature is more beneficial to the adsorption of berberine on SiO<sub>2</sub>@C- $\pi$ -CP.

### Thermodynamic studies

According to the analysis in adsorption isotherms, they clearly indicate that within the range of test, the adsorption capacity changes with temperature. The following thermodynamic equations are used to calculate thermodynamic parameters, including standard free energy change ( $\Delta G^0$ ), standard entropy change ( $\Delta S^0$ ), and standard enthalpy change ( $\Delta H^0$ ):

$$\ln K_d = \Delta S^0 / R - \Delta H^0 / (RT) \quad (7)$$

$$\Delta G^0 = \Delta H^0 - T \Delta S^0 \quad (8)$$

Here, the  $K_d$  obtained by plotting the  $\ln(q_e/C_e)$  against  $q_e$  (Fig. S2(a)) is the thermodynamic equilibrium constant;  $T$  (K) is the temperature of berberine absolute. The  $\Delta H^0$  and  $\Delta S^0$  values can be calculated by the slope and intercept of the linear regression equation of  $1/T$  versus  $\ln K_d$  (Fig. S2(b)).

The fitted thermodynamic data are listed in Table 3. The negative values of  $\Delta G^0$  state that the adsorption process is spontaneous, which means that the adsorption occurs without any external energy source, and the degree of spontaneity of the adsorption reaction decreased by increasing temperature [33]. The values of  $\Delta G^0$  (from -6.778 to -7.226 J mol<sup>-1</sup>) are all higher than -20 kJ mol<sup>-1</sup>, which means that the adsorption is a physical adsorption process. The negative values of  $\Delta H^0$  show that the adsorption process is exothermic, suggesting that the adsorption capacity should decrease with the increase in temperature. It is consistent with the analysis result of the adsorption isotherm part. Also, the absolute value of  $\Delta H^0$  (0.003 J mol<sup>-1</sup>) is less than 40 kJ mol<sup>-1</sup>, which indicates that the adsorption process is physical adsorption, consistent



**Table 2** Parameters of different isotherm models at different temperatures for berberine adsorption on SiO<sub>2</sub>@C-π-CP

Different temperatures (K)	Langmuir			Freundlich			Temkin		
	$K_L$ (L mg <sup>-1</sup> )	$q_{max}$ (mg g <sup>-1</sup> )	$R^2$	$K_F$ (mg g <sup>-1</sup> (mg L <sup>-1</sup> ) <sup>-1/n</sup> )	$1/n$	$R^2$	$K_T$ (L mg <sup>-1</sup> )	$b$ (kJ mol <sup>-1</sup> )	$R^2$
303	1.736	15.698	0.986	9.988	0.131	0.821	577.612	1.583	0.878
313	0.826	14.204	0.928	8.239	0.148	0.859	121.744	1.562	0.892
323	0.427	13.812	0.976	7.093	0.165	0.816	45.349	1.548	0.848

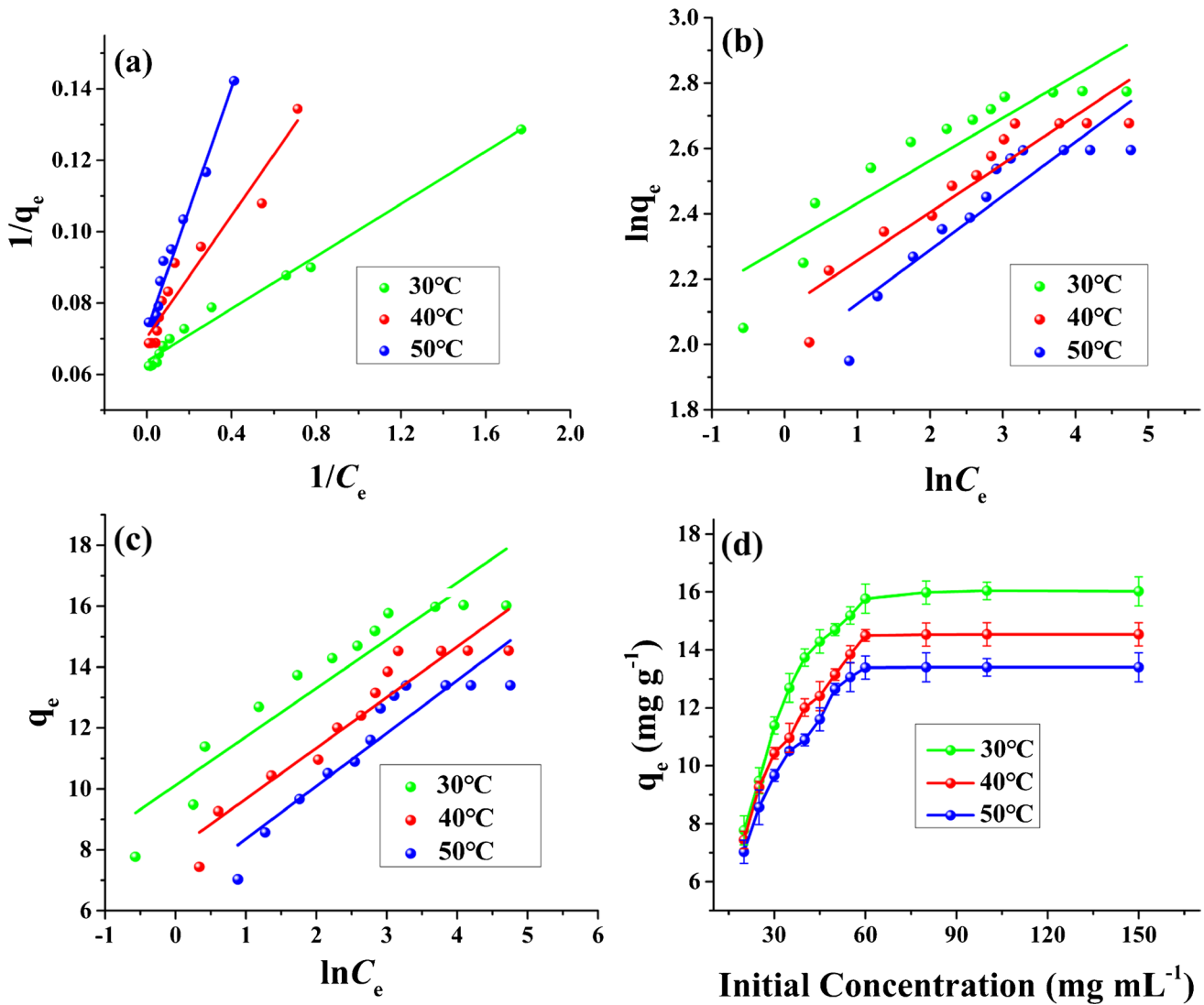


**Fig. 5** The adsorption isotherms of berberine at different temperatures onto SiO<sub>2</sub>@C-π-CP fitted by Langmuir model (a), Freundlich model (b), and Temkin model (c). Effect of initial concentration on the adsorption of berberine at different temperatures onto SiO<sub>2</sub>@C-π-CP (d)

with the results of the  $\Delta G^0$  values. The value of  $\Delta S^0$  is positive, indicating that during the adsorption of berberine on the surface of SiO<sub>2</sub>@C-π-CP, the entropy of the system increases, which means that the randomness of the solid-liquid interface increases. This is because during the adsorption progress, both

solute and solvent would be adsorbed. The adsorption of solute is a process of entropy reduction, accompanied by solvent desorption which is a process of entropy increase. The entropy change in the adsorption process is the result of a comprehensive interaction [36].

**Table 3** Thermodynamic parameters for berberine adsorption on  $\text{SiO}_2@\text{C}-\pi\text{-CP}$  under different temperatures

Temperatures (K)	$K_d$	$\ln K_d$	$\Delta G^0$ (J mol <sup>-1</sup> )	$\Delta H^0$ (J mol <sup>-1</sup> )	$\Delta S^0$ (J mol K <sup>-1</sup> )
303	5.726	1.745	-6.778	-0.003	0.022
313	4.497	1.503	-7.002		
323	3.191	1.160	-7.226		

## Optimization of SPE parameters

### Effect of loading volume

During the SPE process, as the volume of the loading solution increased, the adsorption sites were gradually saturated, and the adsorption capacity of the adsorbent to the sample gradually decreased. So, it is very necessary to know the optimal loading volume. In this work, a  $10 \mu\text{g mL}^{-1}$  berberine solution was used as the sample loading solution. As shown in Fig. 6a, when the loading volume reaches 16 mL, the recoveries only show a slight downward trend, which is basically close to complete adsorption ( $\geq 98.6\%$ ). When the loading volume exceeds 16 mL, the recoveries continue to decrease significantly. Therefore, when a  $10 \mu\text{g mL}^{-1}$  berberine solution is used as the sample loading solution, the corresponding optimal sample loading volume is 16 mL.

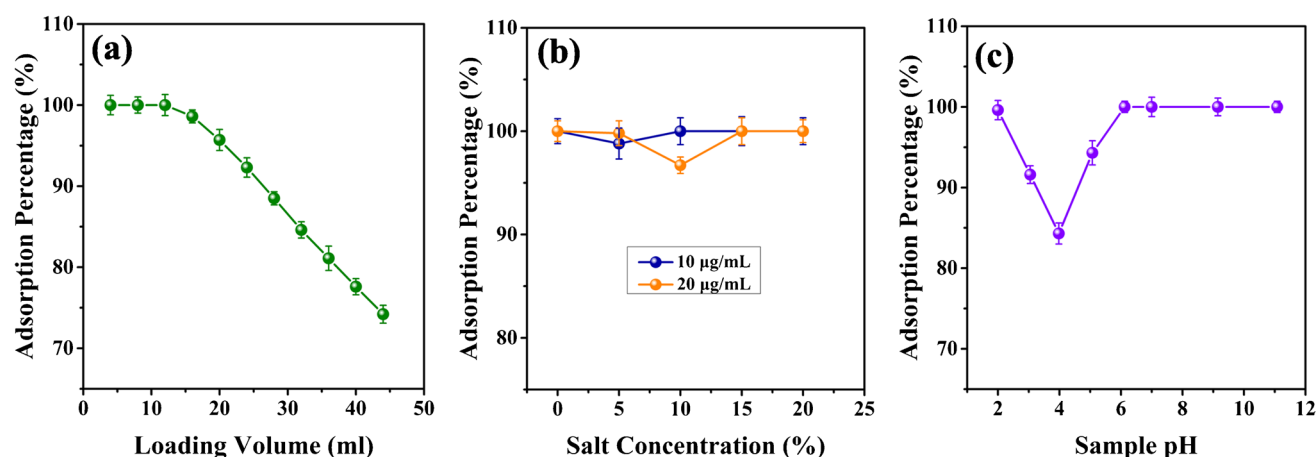
### Effect of salt concentration

The same material may have completely different adsorption behaviors in the loading system with different salt concentrations. The salt concentration mainly affects the adsorption by changing the interaction environment. In this research, five NaCl concentrations (0, 5%, 10%, 15%,

and 20%) were set. As shown in Fig. 6b, when the loading concentration is  $10 \mu\text{g mL}^{-1}$ , the recoveries remain unchanged as the salt concentration increases. However, when the loading concentration increased to  $20 \mu\text{g mL}^{-1}$ , as the salt concentration increased, the recoveries first decreased and then increased, but all still maintain at a high level ( $\geq 96.7\%$ ). By heat treatment,  $\text{SiO}_2@\text{C}-\pi\text{-CP}$  has abundant surface conjugation. When the loading sample concentration was only  $10 \mu\text{g mL}^{-1}$ , the amount of analyte was much lower than the adsorption capacity of adsorbent, and the analyte can be completely adsorbed only by conjugation interaction; therefore, the salt did not cause the recoveries changes. When the loading concentration increased to  $20 \mu\text{g mL}^{-1}$ , it was difficult to achieve complete analyte adsorption only by conjugation interaction; therefore, as the salt concentration increases, the recoveries gradually decrease. However, as the salt concentration continues to increase, the ion concentration in the solution continues to increase. At this moment, the solution environment was more inclined to reduce the ion concentration and “drive out” the analyte, which was manifested as an increase in the recoveries. So, taken together, 0% was selected as the best salt concentration.

### Effect of sample pH

The pH value of sample solution determines the ionization state of analyte, which may affect the adsorption capacity. So, in this work, different pH conditions (pH 2 to 11) were investigated, and the results are shown in Fig. 6c. From pH 2 to 5, the recoveries first decrease and then increase. When  $\text{pH} \geq 6$ , the recoveries reach 100% and no longer change. After high-temperature carbonization treatment, the polar groups of  $\pi\text{-CP}$  shell sharply decrease, and the proportion of conjugated structures is greatly increased. Conjugation became the main interaction between C- $\pi\text{-CP}$  shell and

**Fig. 6** Effects of cumulative volume (a), salt concentration (b), and pH of loading sample (c) on extraction efficiency

berberine, which is less affected by pH changes. At the same time, heat treatment also made the isoelectric point ( $pI$ ) of the polymer lower (drops to  $\sim 4$ ). When the pH of the sample solution changes around the isoelectric point, the charges on  $\text{SiO}_2@\text{C}-\pi\text{-CP}$  surface change accordingly [37]. This is the reason why the change in recoveries occurs only around 4. In order to simplify the subsequent experiment operation, pH 6 was selected as the best sample pH, that is, pure water was used as the sample medium.

### Effect of organic solvent type

It can be seen from the effect of sample pH that the interaction between  $\text{SiO}_2@\text{C}-\pi\text{-CP}$  and berberine is affected by the pH value of the adsorption environment. Therefore, the elution efficiencies of methanol (MeOH), ethanol (EtOH),

acetonitrile (ACN), acetone (Ac), and isopropanol (IPA) were all tested under two different pH conditions. Figure 7a shows that among the two groups of pH conditions and five eluents investigated, the recovery of the ethanol solution at pH 3 is the highest.

### Effect of ethanol and water ratio

Under certain conditions, a certain proportion of water may enhance the elution efficiency of eluents. Therefore, after determining that ethanol was the most suitable organic solvent, a series of ethanol–water solutions with different volume ratios (adjusted to pH 3 with phosphoric acid) were investigated. From the results shown in Fig. 7b, we can clearly see that the recoveries are highest when pure ethanol or ethanol–water solution with a volume ratio of 4:1 is used as the eluent. Then, as the water phase ratio continues

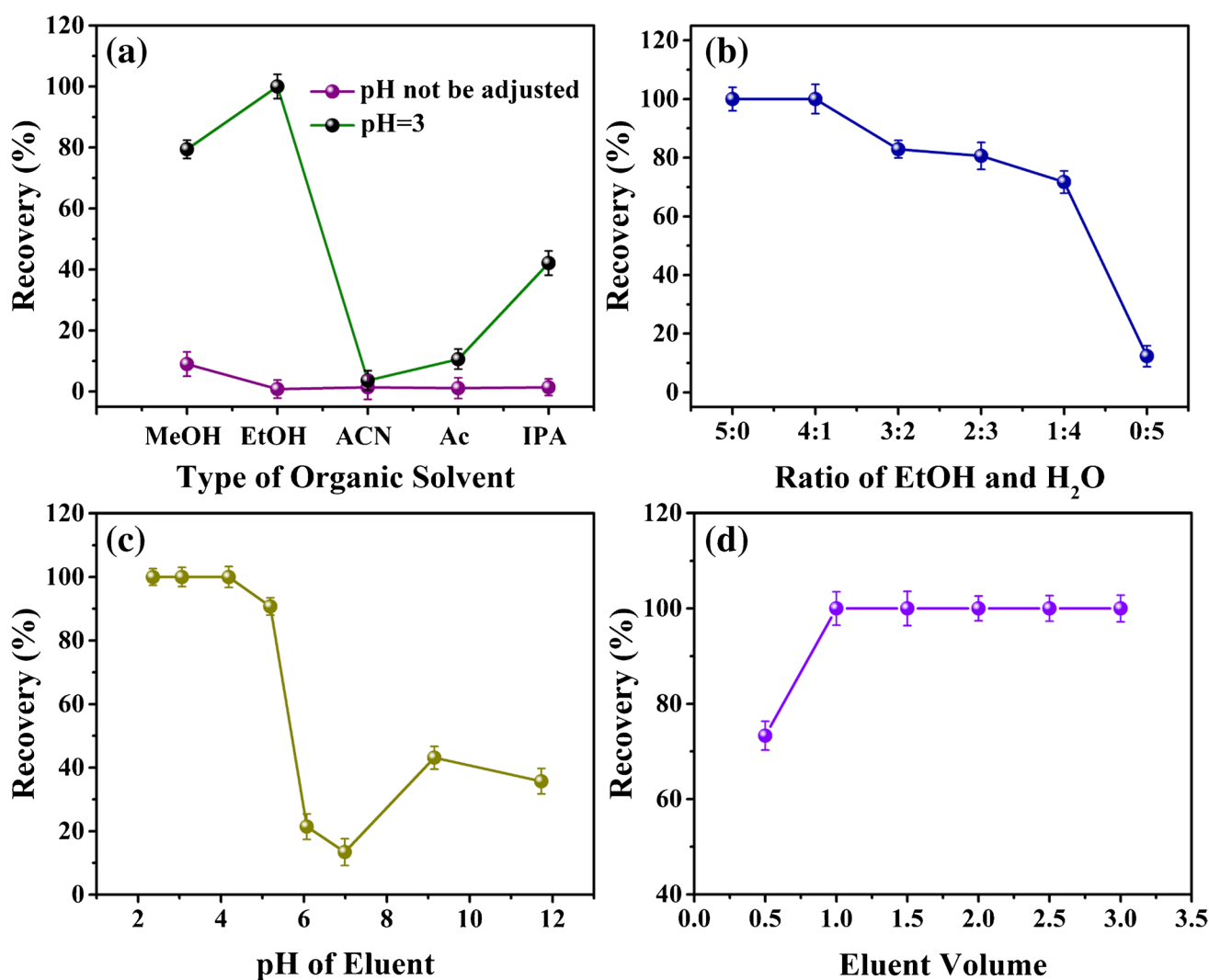


Fig. 7 Effects of organic solvent type (a), ethanol and water ratio (b), pH of eluent (c), and elution volume (d) on extraction efficiency

to increase, the recoveries decline. This is because the main force between berberine and the adsorbent is conjugation interaction. Also, ethanol is less polar than water; so, it is easier to “peel” berberine from  $\text{SiO}_2@\text{C}-\pi\text{-CP}$ . Based on the considerations of green scientific research and easy-to-adjust pH, the ethanol–water solution with a volume ratio of 4:1 was the best, finally.

### Effect of eluent pH

The elution effect is affected by the pH value of the eluent. The recoveries of eluents with different pH values showed obvious differences. In this work, the pHs ranging from 2.4 to 11.7 were conducted. As shown in Fig. 7c, when the pH values are in the range of 2.4 to 4.2, the recoveries are all maintained at a relatively high level. When the pH values are higher than 5.2, the recoveries begin to drop sharply and then up and down again. This is because pH changes could cause simultaneously changes in the charge on  $\text{SiO}_2@\text{C}-\pi\text{-CP}$  surface and the form of berberine present. When the pH value of eluent is higher than *pI* (about 4), the charge on  $\text{SiO}_2@\text{C}-\pi\text{-CP}$  is mainly negative, enhanced the electrostatic interaction between berberine and  $\text{SiO}_2@\text{C}-\pi\text{-CP}$ , and impeded elution. When the alkalinity of the solution increases, part of the berberine will change from the hydrophilic quaternary ammonium form to the lipophilic aldehyde or alcohol form. The combined effect of these two results in abnormal fluctuations in recovery. Finally, considering that the hydrolysis of  $\text{SiO}_2$  will be enhanced under strong acidic conditions, pH 4 was selected as the optimal pH condition for elution.

### Effect of elution volume

Based on the consideration of elution efficiency, it is necessary to explore a proper eluent volume. So, this work investigated the effect of elution volume in the range of 0.5–3 mL. The results in Fig. 7d show that 1 mL of eluent is sufficient to achieve complete elution, so 1 mL was chosen as the optimal elution volume.

### Reusability of $\text{SiO}_2@\text{C}-\pi\text{-CP}$

The reusability of  $\text{SiO}_2@\text{C}-\pi\text{-CP}$  was tested under the optimal SPE conditions, and the results are shown in Fig. S3.  $\text{SiO}_2@\text{C}-\pi\text{-CP}$  still maintained satisfactory recoveries of berberine even after 12 cycles of use. The recoveries in the whole process were maintained above 99%, indicating that the physical structure and chemical properties of  $\text{SiO}_2@\text{C}-\pi\text{-CP}$  have high stability.

### Method validation for $\text{SiO}_2@\text{C}-\pi\text{-CP}$

Under the optimal SPE conditions, the method validation of the SPE-HPLC/DAD analysis method based on  $\text{SiO}_2@\text{C}-\pi\text{-CP}$  adsorbent had been completed. Good linearities were obtained in the range of 2–13,000  $\text{ng mL}^{-1}$  for berberine with correlation coefficients better than 99.3%. LODs (signal/noise = 3) and LOQs (signal/noise = 10) were 0.75  $\text{ng mL}^{-1}$  and 2  $\text{ng mL}^{-1}$ , respectively. Intra-day ( $n=3$ ) and inter-day ( $n=6$ ) repeatability were tested to determine the method precision. The RSDs of inter-day and intra-day were 1.5% and 6.2%, respectively. These above data could show that the method proposed in this work is effective and reliable.

### Application in real sample

In order to verify whether the method established above is applicable to the analysis of actual samples, the content of berberine in human urine was determined in this test [38]. From the chromatograms in Fig. 8 and results listed in Table S4, it can be clearly seen that the enrichment of trace berberine in human urine samples can be achieved by this established SPE method. In Fig. 8, no peaks of the berberine were observed in blank human urine solution whether with SPE or not. Also, for the spiked urine solution, the obvious peak of berberine is also only seen after SPE. Besides, the recoveries are all very satisfactory (98–103%) with RSD ( $n=3$ ) less than 5%. These all indicate that  $\text{SiO}_2@\text{C}-\pi\text{-CP}$  can resist interference from the urine matrix.

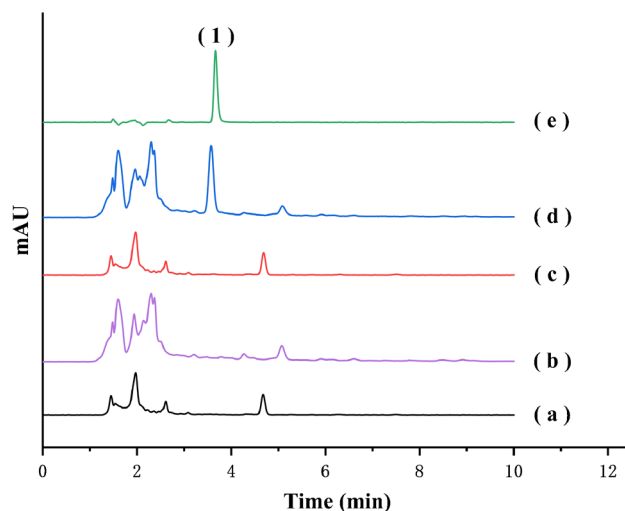


**Fig. 8** Chromatograms of (I) berberine. (a) Blank human urine. (b) Blank human urine by SPE. (c) Human urine spiked with berberine at 75  $\text{ng mL}^{-1}$ . (d) Real human urine sample spiked at 75  $\text{ng mL}^{-1}$  by SPE. (e) Berberine standard solution at a concentration of 10  $\mu\text{g mL}^{-1}$

**Table 4** Comparison of the proposed method with other extraction techniques for determination of berberine in different real samples

Adsorbent materials	Analytical methods	Linear range	LODs	Real sample	Recovery (%)	Ref
Berberine-imprinted monolith	MI- $\mu$ -SPE-HPLC/UV	3–800 ng mL <sup>-1</sup>	1.0 ng mL <sup>-1</sup>	Human plasma and urine	90.6–103.2	[39]
TSPSACide@GO/SiO <sub>2</sub>	SPE-HPLC/UV	2–100 $\mu$ g L <sup>-1</sup>	1 $\mu$ g L <sup>-1</sup>	Human urine	81.3	[19]
Berberine M-MIPs	M-MI-SPE-HPLC/UV	0.1–150 ng mL <sup>-1</sup>	0.01 ng mL <sup>-1</sup>	<i>Cortex phellodendri</i> and rat plasma	94.07–99.95	[40]
PNB-MNPs	UADM-SPE-HPLC/UV	–	0.17–0.19 ng mL <sup>-1</sup>	Human plasma and urine	93.9–94.7	[42]
Aptamer-functionalized Fe <sub>3</sub> O <sub>4</sub> MNPs	MAPE-HPLC/UV	–	–	<i>C. phellodendri</i> extracts	95.4–111.3	[43]
GO-modified monolithic syringe	SPE-HPLC/UV	1–50 $\mu$ g L <sup>-1</sup>	0.5 $\mu$ g L <sup>-1</sup>	HLSQ pills	85.6	[22]
HP- $\beta$ -CD	Mini-SPE-UHPLC-Q-TOF/MS	–	–	River water, orange juice, and tomato juice	88.3–93.2	[47]
SDS-coated Fe <sub>3</sub> O <sub>4</sub> NPs	Dispersive admicelle SPE-HPLC/UV	0.003–3 $\mu$ g mL <sup>-1</sup>	0.49 ng mL <sup>-1</sup>	Gegen-Qinlian oral liquid	87.9–96.4	[44]
T-MIR	Thermal-assisted DSPE-HPLC/UV	0.1–100.0 mg L <sup>-1</sup>	0.008 mg L <sup>-1</sup>	A real plant	–	[41]
Ni@POFs	MSPE-UPLC-MS/MS	0.02–20 ng mL <sup>-1</sup>	0.006 ng mL <sup>-1</sup>	Patient's urine	95.8–97.8	[18]
UiO-66@PA@PEI@Fe <sub>3</sub> O <sub>4</sub>	MSPE-HPLC/UV	1.375–185 $\mu$ g mL <sup>-1</sup>	–	<i>Coptis chinensis</i> and <i>Phellodendron amurense</i>	71.6–76.1	[45]
Fe <sub>3</sub> O <sub>4</sub> @YS-UiO-66-NH <sub>2</sub>	MSPE-HPLC/UV	0.048–200 $\mu$ g mL <sup>-1</sup>	3.13 ng mL <sup>-1</sup>	Rat plasma	89.9–93.1	[46]
SiO <sub>2</sub> @C- $\pi$ -CP	SPE-HPLC/UV	2–13,000 ng mL <sup>-1</sup>	0.75 ng mL <sup>-1</sup>	Human urine	98.1–98.8	This work

## Comparison with other extraction methods

Berberine is a commonly used drug in clinical treatment. It is very necessary to realize the accurate determination of trace berberine in clinical samples. Faced with this demand, combined with the high-efficiency sample pretreatment technology (SPE), a series of novel adsorption materials were developed by researchers to analyze berberine. They include customized imprinted materials [39–41], which were designed and synthesized to achieve precise identification and detection; magnetic SPE materials [18, 40, 42–46] that were introduced into the analysis system for reaching rapid solid–liquid separation during the extraction process; and other composite materials [19, 22, 47].

Most of the above-developed analytical methods have achieved satisfactory analysis efficiency, but the synthesis process of these adsorbent materials was all not simple, and some of them used LC/MS testing techniques that are not yet widely popularized in domestic small and medium-sized enterprises, which is very likely to restrict the promotion and application of analysis method.

By comparison, the synthesis process of the SiO<sub>2</sub>@C- $\pi$ -CP adsorbent used in this work is very economical and the liquid chromatography detection technology used is very popular, easy to implement, and highly accurate. Moreover, the detection limit and linear range also have absolute advantages. Therefore, compared with these existing berberine adsorbents, SiO<sub>2</sub>@C- $\pi$ -CP is more suitable for the actual clinical analysis process and has greater potential for commercial development. More detailed comparison is summarized in Table 4.

## Conclusions

In this paper, based on a novel  $\pi$ -conjugated polymer, a SPE adsorbent SiO<sub>2</sub>@C- $\pi$ -CP with great commercial potential was designed and successfully synthesized. Combined with HPLC/DAD, SiO<sub>2</sub>@C- $\pi$ -CP can achieve accurate determination of trace berberine in complex matrices. Compared with the reported adsorbents for berberine analysis, SiO<sub>2</sub>@C- $\pi$ -CP has a simpler synthesis process, wider detection range, excellent enrichment effect, and recycling and anti-interference ability. It is precisely because SiO<sub>2</sub>@C- $\pi$ -CP has these advantages that it is very likely to go out of the laboratory and achieve commercial production, breaking the shackles of existing materials that are difficult to achieve market transformation. This work opens a novel method for efficient determination of berberine; it is also clarified that there is a possibility of commercial application of the  $\pi$ -CP in berberine alkaloids sample pretreatment, which would open up a new direction for the application of these highly economical  $\pi$ -conjugated polymers.



**Supplementary Information** The online version contains supplementary material available at <https://doi.org/10.1007/s00604-022-05496-y>.

**Funding** This work was financially supported by the National Natural Science Foundation of China (Grant No. 22104071) and the Natural Science Foundation of Shandong Province of China (Grant No. ZR2021QB029).

## Declarations

**Conflict of interest** The authors declare no competing interests.

## References

- Kwon M, Lim DY, Lee CH, Jeon J-H, Choi M-K, Song I-S (2020) Enhanced intestinal absorption and pharmacokinetic modulation of berberine and its metabolites through the inhibition of P-glycoprotein and intestinal metabolism in rats using a berberine mixed micelle formulation. *Pharmaceutics* 12:882
- Wang Y, Liu Y, Du X, Ma H, Yao J (2020) The anti-cancer mechanisms of berberine: a review. *Cancer Manage Res* 12:695–702
- Joshi PV, Shirkhedkar AA, Prakash K, Maheshwari VL (2011) Antidiarrheal activity, chemical and toxicity profile of *Berberis aristata*. *Pharm Biol* 49:94–100
- Du GF, Le YJ, Sun X, Yang XY, He QY (2020) Proteomic investigation into the action mechanism of berberine against *Streptococcus pyogenes*. *J Proteomics* 215:103666
- Shao J, Zeng D, Tian S, Liu G, Fu J (2020) Identification of the natural product berberine as an antiviral drug. *AMB Express* 10:164
- Vrzal R, Zdarilova A, Ulrichova J, Blaha L, Giesy JP, Dvorak Z (2005) Activation of the aryl hydrocarbon receptor by berberine in HepG2 and H4IIE cells: biphasic effect on CYP1A1. *Biochem Pharmacol* 70(6):925–936
- Milata V, Svedova A, Barbierikova Z, Holubkova E, Cipakova I, Cholujovala D, Jakubikova J, Panik M, Jantova S, Brezova V, Cipak L (2019) Synthesis and anticancer activity of novel 9-O-substituted berberine derivatives. *Int J Mol Sci* 20:2169
- Yin J, Hou Y, Yin Y, Song X (2017) Selenium-coated nanostructured lipid carriers used for oral delivery of berberine to accomplish a synergic hypoglycemic effect. *Int J Nanomed* 12:8671–8680
- Cheng Z, Liu S, Wu X, Raza F, Li Y, Yuan W, Qiu M, Su J (2020) Autologous erythrocytes delivery of berberine hydrochloride with long-acting effect for hypolipidemia treatment. *Drug Delivery* 27:283–291
- Liu M, Zhu D, Wen J, Ding W, Huang S, Xia C, Zhang H, Xiong Y (2020) Berberine promotes OATP1B1 expression and rosuvastatin uptake by inducing nuclear translocation of FXR and LXRalpha. *Front Pharmacol* 11:375
- Kuo CL, Chi CW, Liu TY (2004) The anti-inflammatory potential of berberine in vitro and in vivo. *Cancer Lett* 203:127–137
- Wang Z, Chen Z, Yang S, Wang Y, Huang Z, Gao J, Tu S, Rao Z (2014) Berberine ameliorates collagen-induced arthritis in rats associated with anti-inflammatory and anti-angiogenic effects. *Inflammation* 37:1789–1798
- Laudadio E, Cedraro N, Mangiaterra G, Citterio B, Mobbili G, Minnelli C, Bizzaro D, Biavasco F, Galeazzi R (2019) Natural alkaloid berberine activity against *Pseudomonas aeruginosa* MexXY-mediated aminoglycoside resistance: in silico and in vitro studies. *J Nat Prod* 82:1935–1944
- Zhang L, Wu X, Yang R, Chen F, Liao Y, Zhu Z, Wu Z, Sun X, Wang L (2020) Effects of berberine on the gastrointestinal microbiota. *Front Cell Infect Microbiol* 10:588517
- Zhu D, Li W, Wen H-M, Hu Y, Wang J, Zhu J-M, Ni W-T, Gu C-Q (2015) Development of polyacrylic acid-functionalized porous zinc sulfide nanospheres for a non-aqueous solid phase extraction procedure toward alkaloids. *RSC Adv* 5:29820–29827
- Sadanala KC, Chung BC (2013) Graphene nanoplatelets as a solid phase extraction sorbent for analysis of chlorophenols in water. *J Korean Soc Appl Biol Chem* 56:673–678
- Li G, Wang X, Row KH (2017) Magnetic solid-phase extraction with Fe<sub>3</sub>O<sub>4</sub>/molecularly imprinted polymers modified by deep eutectic solvents and ionic liquids for the rapid purification of alkaloid isomers (theobromine and theophylline) from *Green Tea*. *Molecules* 22:1061
- Hu K, Pang T, Shi Y, Cheng J, Huang Y (2020) Facile preparation of a magnetic porous organic frameworks for highly sensitive determination of eight alkaloids in urine samples based UHPLC-MS/MS. *Microchem J* 157:105048
- Liu H, Guo Y, Wang X, Li Y, Liang X, Liu X (2015) Double carboxyl silicane modified graphene oxide coated silica composite as sorbent for solid-phase extraction of quaternary alkaloids. *Anal Methods* 7:135–142
- Murakami A, Noguchi H, Kuwahara Y, Takafuji M, Nozato S, Sun R-d, Nakasuga A, Ihara H (2017) Non-conductive, size-controlled monodisperse black particles prepared by a one-pot polymerization and low-temperature calcination. *Chem Lett* 46:680–682
- Ye N, Li J, Gao C, Xie Y (2013) Simultaneous determination of atropine, scopolamine, and anisodamine in *Flos datuarae* by capillary electrophoresis using a capillary coated by graphene oxide. *J Sep Sci* 36:2698–2702
- Liang X, Wang L, Wang S, Li Y, Guo Y (2017) Direct preparation of a graphene oxide modified monolith in a glass syringe as a solid-phase extraction cartridge for the extraction of quaternary ammonium alkaloids from Chinese patent medicine. *J Sep Sci* 40:4411–4419
- Mehranfar A, Izadyar M, Shamkhali AN (2018) A joint MD/QM study on the possibility of alkaloids detection by cucurbiturils and graphene oxide-cucurbituril composites. *J Mol Liq* 272:963–972
- Khan MN, Orimoto Y, Ihara H (2018) Amphiphilic spherical nanoparticles with a nitrogen-enriched carbon-like surface by using  $\beta$ -lactoglobulin as a template. *Chem Commun* 54:13204–13207
- Noguchi H, Sultana M, Hano N, Kuwahara Y, Takafuji M, Nagaoka S, Qiu H, Ihara H (2020) Fabrication of carbon-like,  $\pi$ -conjugated organic layer on a nano-porous silica surface. *Nanomaterials* 10:1882
- Noguchi H, Liu T, Nozato S, Kuwahara Y, Takafuji M, Nagaoka S, Ihara H (2017) Novel black organic phase for ultra selective retention by surface modification of porous silica. *Chem Lett* 46:1233–1236
- Guo Q, Liu D, Zhang X, Li L, Hou H, Niwa O, You T (2014) Pd-Ni alloy nanoparticle/carbon nanofiber composites: preparation, structure, and superior electrocatalytic properties for sugar analysis. *Anal Chem* 86:5898–5905
- Ababneh H, Hameed BH (2021) Chitosan-derived hydrothermally carbonized materials and its applications: a review of recent literature. *Int J Biol Macromol* 186:314–327
- Chen Y, Liu B, Chen Z, Zuo X (2021) Innovative electrochemical sensor using TiO<sub>2</sub> nanomaterials to detect phosphopeptides. *Anal Chem* 93:10635–10643
- Soltani R, Marjani A, Shirazian S (2019) Facile one-pot synthesis of thiol-functionalized mesoporous silica submicrospheres for Tl(I) adsorption: isotherm, kinetic and thermodynamic studies. *J Hazard Mater* 371:146–155

31. Khandaker S, Toyohara Y, Kamida S, Kuba T (2018) Effective removal of cesium from wastewater solutions using an innovative low-cost adsorbent developed from sewage sludge molten slag. *J Environ Manage* 222:304–315
32. Li Y, Yuan B, Fu J, Deng S, Lu X (2013) Adsorption of alkaloids on ordered mesoporous carbon. *J Colloid Interface Sci* 408:181–190
33. Argun ME, Güçlü D, Karatas M (2014) Adsorption of Reactive Blue 114 dye by using a new adsorbent: pomelo peel. *J Ind Eng Chem* 20:1079–1084
34. Mirsoleimani-azizi SM, Setoodeh P, Zeinali S, Rahimpour MR (2018) Tetracycline antibiotic removal from aqueous solutions by MOF-5: adsorption isotherm, kinetic and thermodynamic studies. *J Environ Chem Eng* 6:6118–6130
35. Ghanei M, Rashidi A, Tayebi H-A, Yazdanshenas ME (2018) Removal of Acid Blue 25 from aqueous media by magnetic-SBA-15/CPAA super adsorbent: adsorption isotherm, kinetic, and thermodynamic studies. *J Chem Eng Data* 63:3592–3605
36. Bekçi Z, Seki Y, Kadir Yurdakoç M (2007) A study of equilibrium and FTIR, SEM/EDS analysis of trimethoprim adsorption onto K10. *J Mol Struct* 827:67–74
37. Hano N, Takafuji M, Noguchi H, Ihara H (2019) Monodisperse surface-charge-controlled black nanoparticles for near-infrared shielding. *ACS Appl Nano Mater* 2:3597–3605
38. Pan J, Yu C, Zhu D, Zhang H, Zeng J, Jiang S, Ren J (2002) Identification of three sulfate-conjugated metabolites of berberine chloride in healthy volunteers' urine after oral administration. *Acta Pharmacol Sin* 23:77–82
39. Zhang W, Chen Z (2013) Preparation of micropipette tip-based molecularly imprinted monolith for selective micro-solid phase extraction of berberine in plasma and urine samples. *Talanta* 103:103–109
40. Meng J, Zhang W, Bao T, Chen Z (2015) Novel molecularly imprinted magnetic nanoparticles for the selective extraction of protoberberine alkaloids in herbs and rat plasma. *J Sep Sci* 38:2117–2125
41. Tang W, Row KH (2018) Novel controllable hydrophilic thermo-responsive molecularly imprinted resin adsorbent prepared in water for selective recognition of alkaloids by thermal-assisted dispersive solid phase extraction. *J Pharm Biomed Anal* 160:386–396
42. Aghaie ABG, Hadjmohammadi MR (2016) Fe<sub>3</sub>O<sub>4</sub>@p-Naphtholbenzein as a novel nano-sorbent for highly effective removal and recovery of berberine: response surface methodology for optimization of ultrasound assisted dispersive magnetic solid phase extraction. *Talanta* 156–157:18–28
43. Jiang LF, Chen BC, Chen B, Li XJ, Liao HL, Zhang WY, Wu L (2017) Aptamer-functionalized Fe<sub>3</sub>O<sub>4</sub> magnetic nanoparticles as a solid-phase extraction adsorbent for the selective extraction of berberine from *Cortex phellodendri*. *J Sep Sci* 40:2933–2940
44. Shi Z, Xu D, Zhao X, Li X, Shen H, Yang B, Zhang H (2017) Dispersive admicelle solid-phase extraction based on sodium dodecyl sulfate coated Fe<sub>3</sub>O<sub>4</sub> nanoparticles for the selective adsorption of three alkaloids in Gegen-Qinlian oral liquid before high-performance liquid chromatography. *J Sep Sci* 40:4591–4598
45. Wang Y, Yin SJ, Zhao CP, Chen GY, Yang FQ (2021) Preparation of a zirconium terephthalate metal-organic framework coated magnetic nanoparticle for the extraction of berberine prior to high-performance liquid chromatography analysis. *J Sep Sci* 44:1220–1230
46. Yin SJ, Wang X, Jiang H, Lu M, Zhou X, Li LX, Yang FQ (2021) Preparation of magnetic yolk-shell structured metal-organic framework material and its application in pharmacokinetics study of alkaloids. *Anal Bioanal Chem* 413:6987–6999
47. Peng LQ, Ye LH, Cao J, Chang YX, Li Q, An M, Tan Z, Xu JJ (2017) Cyclodextrin-based miniaturized solid phase extraction for biopesticides analysis in water and vegetable juices samples analyzed by ultra-high-performance liquid chromatography coupled with quadrupole time-of-flight mass spectrometry. *Food Chem* 226:141–148

**Publisher's note** Springer Nature remains neutral with regard to jurisdictional claims in published maps and institutional affiliations.

Springer Nature or its licensor holds exclusive rights to this article under a publishing agreement with the author(s) or other rightsholder(s); author self-archiving of the accepted manuscript version of this article is solely governed by the terms of such publishing agreement and applicable law.